



# Preparation and characterization of magnetic nanocomposite of Schiff base/silica/magnetite as a preconcentration phase for the trace determination of heavy metal ions in water, food and biological samples using atomic absorption spectrometry

Hasan Bagheri<sup>a</sup>, Abbas Afkhami<sup>b,\*</sup>, Mohammad Saber-Tehrani<sup>a</sup>, Hosein Khoshshafar<sup>b</sup>

<sup>a</sup> Department of Chemistry, Science and Research Branch, Islamic Azad University, Tehran, Iran

<sup>b</sup> Faculty of Chemistry, Bu-Ali Sina University, Hamedan, Iran

## ARTICLE INFO

### Article history:

Received 22 February 2012

Received in revised form

24 March 2012

Accepted 28 March 2012

Available online 24 April 2012

### Keywords:

Preconcentration

Atomic absorption spectrometric

determination

Solid phase extraction

Magnetic nanoparticles

## ABSTRACT

A versatile and robust solid phase with both magnetic property and a very high adsorption capacity is presented on the basis of modification of iron oxide-silica magnetic particles with a newly synthesized Schiff base ( $\text{Fe}_3\text{O}_4/\text{SiO}_2/\text{L}$ ). The structure of the resulting product was confirmed by Fourier transform infrared (FT-IR) spectra, X-ray diffraction (XRD) spectrometry and transmission electron microscopy (TEM). We developed an efficient and cost-effective method for the preconcentration of trace amounts of Pb(II), Cd(II) and Cu(II) in environmental and biological samples using this novel magnetic solid phase. Prepared magnetic solid phase is an ideal support because it has a large surface area, good selectivity and can be easily retrieved from large volumes of aqueous solutions. The possible parameters affecting the enrichment were optimized. Under the optimal conditions, the method detection limit was 0.14, 0.19 and  $0.12 \mu\text{g L}^{-1}$  for Pb(II), Cd(II) and Cu(II) ions, respectively. The established method has been successfully applied to analyze real samples, and satisfactory results were obtained. All these indicated that this magnetic phase had a great potential in environmental and biological fields.

© 2012 Elsevier B.V. All rights reserved.

## 1. Introduction

Interest in monitoring toxic metal ions in aquatic ecosystems still continues as these contaminants adversely affect the environment and have serious medical effects. The World Health Organization (WHO) estimates that about 25% of the diseases facing humans today occur due to long-term exposure to environmental pollution, including air, soil, and water pollution [1]. Improper management of industrial water is one of the main causes of environmental pollution and degradation in many countries. Heavy metals are important species in these wastes and harmful to plants and animals.

Heavy metals show a great tendency to form complexes, especially with ligands of biological matters containing nitrogen, sulfur, and oxygen. As a result, changes in the molecular structure of proteins, breaking of hydrogen bonds, or inhibition of enzymes may occur. These interactions, among others, may explain the toxicological and carcinogenic effects of heavy metals such as those affecting the central nervous system (Hg(II), Pb(II), As(III)); the kidneys or liver (Cu(II), Cd(II), Hg(II), Pb(II)); or skin, bones, or

teeth (Ni(II), Cu(II), Cd(II), Cr(III)) [2–4]. Therefore, it is desired to develop simple, selective, efficient and eco-friendly methods for the extraction and analysis of trace amounts of heavy metals in environmental and biological samples [5].

In spite of great improvements in sensitivity and selectivity of modern analytical detection systems, due to the complexity and low concentration of these ions in some samples, separation techniques such as precipitation, solvent extraction, ion exchange etc. are still used to overcome matrix interference and/or to enhance sensitivity through preconcentration of the analyte [6–10]. However, disadvantages, such as significant chemical additives, solvent losses, large secondary wastes, prefiltration problems, high capital and operational costs and being time consuming, limit the application of these techniques. These problems could be addressed by the development of modular and compact processes that provide adequate separation and preconcentration without complex processes. Solid-phase extraction (SPE) is a routine extraction method for the pre-treatment of samples with complex matrices, because it offers enrichment, high recovery, simplicity, high speed, and low organic solvent consumption as its advantages [11–13].

At present, nanometer materials have become more and more important as solid phases due to their special properties. Although investigations of the surface chemistry of highly dispersed oxides,

\* Corresponding author. Tel./fax: +98 811 8272404.  
E-mail address: afkhami@basu.ac.ir (A. Afkhami).

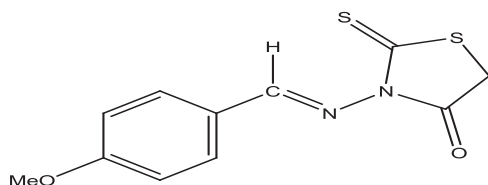
e.g.,  $\text{TiO}_2$ ,  $\text{Al}_2\text{O}_3$ ,  $\text{ZrO}_2$ ,  $\text{SiO}_2$  and  $\text{ZnO}$ , indicated that these materials had very high adsorption capacities [14,15], separation of these particles from aqueous medium is difficult because of very small dimension and high dispersion.

Magnetic nanoparticles (MNPs) with the general formula  $\text{MFe}_2\text{O}_4$  ( $\text{M}=\text{Fe}$ ,  $\text{Co}$ ,  $\text{Cu}$ ,  $\text{Mn}$ , etc.) such as magnetite ( $\text{Fe}_3\text{O}_4$ ), maghemite ( $\gamma\text{-Fe}_2\text{O}_3$ ), and cobalt oxide ( $\text{Co}_3\text{O}_4$ ) are of the most popular materials in analytical biochemistry, medicine, removal of heavy metals, and biotechnology, and have been increasingly applied to immobilize proteins, enzymes, and other bioactive agents due to the advantages of easy control and simple separation [16–22]. It is believed that magnetic nanoparticles exhibit the finite-size effect or high ratio of surface-to-volume, resulting in a higher adsorption capacity for metal sorption.  $\text{Fe}_3\text{O}_4$  nanoparticles have attracted particular interest in separation science, because they can be easily isolated using an external magnetic field placed outside of the extraction container [15,16,21,23]. Furthermore, there are no diffusion limitations, since the available surface is totally external as the MNPs are nonporous. Thus, an efficient, economic, scalable and non-toxic synthesis of  $\text{Fe}_3\text{O}_4$  nanoparticles is highly preferred for potential applications and fundamental researches. However, pure magnetic particles are prone to form aggregates and their magnetic properties can be altered in complex environmental and biological systems. To solve the above problems, a suitable protective coating on a magnetic core is often used. Silica has been considered as one of the most ideal shell materials due to its reliable chemical stability, biocompatibility and versatility in surface modification [15,17,21,23]. The core-shell silica magnetic nanoparticles have high surface areas. Hence, silica-coated  $\text{Fe}_3\text{O}_4$  nanoparticles could be used for rapid separation.

Additionally, silica coated magnetic nanoparticles can be fashioned with a wide range of small organic ligands and large biomacromolecules using tools and techniques of surface modification, and giving rise to highly selective heavy-metal ions sensing systems. The synergy of the properties of these materials with those of the mentioned solid phases gives rise to highly sensitive and cost-efficient heavy metals extractors [15,21].

Schiff base functionalized solid phases have been used for preconcentration of metals [13,24,25]. The 3-(4-methoxybenzylideneamino)-2-thioxothiazolidin-4-one (Scheme 1), with one oxygen, two sulfur and two nitrogen donating Schiff base (L) is insoluble in water. It is known that the Schiff base ligands form very stable complexes with transition metal ions.

In this paper, we explored a novel magnetic adsorbent based on the new synthesized Schiff base-functionalized iron oxide-silica ( $\text{Fe}_3\text{O}_4/\text{SiO}_2$ ) hybrids ( $\text{Fe}_3\text{O}_4/\text{SiO}_2/\text{L}$ ) for the preconcentration of  $\text{Pb}(\text{II})$ ,  $\text{Cd}(\text{II})$  and  $\text{Cu}(\text{II})$ . The structure of new sorbent is like the core-shell nanoparticles, in which the structure from inner to outer is sequentially comprised of a magnetic core, passive film of silica, and functional groups of Schiff base. In order to well protect the magnetic core of the sorbent, the magnetic carrier ( $\text{Fe}_3\text{O}_4/\text{SiO}_2$ ) was first formed and then further functionalized to become a Schiff base functionalized sorbent. The advantages of this magnetic adsorbent are as follows: (1) the magnetic core can provide a convenient platform for the facile separation; (2) the silica shell



**Scheme 1.** Structure of 3-(4-methoxybenzylideneamino)-2-thioxothiazolidin-4-one.

can efficiently prevent the aggregation and chemical decomposition of  $\text{Fe}_3\text{O}_4$  in a harsh environment; (3) L is a selective ligand that it possesses favorable structure and numerous functional groups that can be used to improve adsorption capacity compared with unmodified adsorbent.

The physicochemical properties of the sorbent were characterized with TEM, XRD, FT-IR and specific surface area measurement with nitrogen gas (BET method).

## 2. Experimental

### 2.1. Instruments

The concentration of metal ions was determined by flame atomic absorption spectrometry (FAAS) using a Varian model Spect. AA 220 apparatus. The instrumental settings of the manufacturer were followed. FT-IR spectra ( $4000\text{--}400\text{ cm}^{-1}$ ) in KBr were recorded on a Perkin Elmer, spectrum 100, FT-IR spectrometer. The size, morphology and structure of the nanoparticles were characterized by TEM (Philips, CM10, 100 kV). Specific surface area and porosity were defined by  $\text{N}_2$  adsorption-desorption porosimetry (77 K) using a porosimeter (Bel Japan, Inc). The crystal structure of synthesized materials was determined by an XRD (38066 Riva, d/G.Via M. Misone, 11/D (TN) Italy) at ambient temperature. A Metrohm model 713 (Herisau, Switzerland) pH-meter with a combined glass electrode was used for pH measurements. The inductively coupled plasma-optical emission spectrometry (ICP-OES) instrument was used the Jobin-Yvon Emission (JY138 ultrace, France). Details of operating conditions for the determination of ions were as manufacture manual.

### 2.2. Reagents

High purity reagents from Sigma (St. Louis, MO, USA) and Merck (Darmstadt, Germany) were used for the preparation of all standard and sample solutions. Stock solutions were prepared daily from  $\text{Pb}(\text{II})$ ,  $\text{Cd}(\text{II})$  and  $\text{Cu}(\text{II})$  standard solutions of  $1000.0\text{ mg L}^{-1}$  (Merck, Germany) by serial dilution with deionized water. The deionized water was used throughout the study. Tetraethoxysilane (TEOS) was used for the preparation of sorbent.

### 2.3. Synthesis of 3-(4-Methoxybenzylideneamino)-2-thioxothiazolidin-4-one (L)

The Schiff base L was synthesized according to the literature [26]. A solution of *N*-aminorhodanine (2 mmol) in  $\text{CH}_3\text{CN}$  or  $\text{CH}_3\text{OH}$  (10 mL) was treated with 4-methoxybenzaldehyde in a molar ratio of 1:1.5 and the resulting mixture was acidified by 37% hydrochloric acid (3 drops) or acetic acid (8 drops). The reaction mixture was refluxed for eight hours. The solid residue was filtered, washed with cold solvent (10 mL) to afford the product.

### 2.4. Synthesis of magnetite and silica-coated magnetite nanoparticles

The synthesis of nano-sorbent was designed in three sequential steps, including synthesis of magnetite, coating of magnetite nanoparticles with silica film and preparation of L grafted  $\text{Fe}_3\text{O}_4/\text{SiO}_2$ . The step initially began with the formation of the magnetite ( $\text{Fe}_3\text{O}_4$ ) as a magnetic core by means of chemical precipitation. The MNPs were prepared by the conventional co-precipitation method with minor modifications [15,21]. In this method, ultrasonic vibration by an ultrasonic bath was used instead of magnetic stirring.  $\text{FeCl}_3 \cdot 6\text{H}_2\text{O}$  (11.68 g) and  $\text{FeCl}_2 \cdot 4\text{H}_2\text{O}$  (4.30 g) were dissolved in 200 mL deionized water under nitrogen gas in

an ultrasonic bath at 85 °C for a few min which led to smaller and more homogenized particles. Then, 20 mL of 27% NH<sub>3</sub>, which is different from the 15 mL of 20% NH<sub>3</sub> used in Refs. [15,27], was added to the solution. The color of bulk solution changed from orange to black immediately. The magnetite precipitates were washed twice with deionized water and once with 0.02 mol L<sup>-1</sup> sodium chloride. The washed magnetite was stored in deionized water at a concentration of 40.0 g L<sup>-1</sup>. A silica film was further coated on the magnetic core to compose a magnetic carrier (Fe<sub>3</sub>O<sub>4</sub>/SiO<sub>2</sub>).

Before the further functionalization step, the magnetic core was ensured to be well protected by the silica film. Then, the magnetite suspension prepared above (20 mL) was placed in a 250 mL round-bottom flask and was allowed to settle. The supernatant was removed, and an aqueous solution of tetraethoxysilane [TEOS, 15% (v/v), 80 mL] was added, followed by glycerol (60 mL). The pH of the suspension was adjusted to 4.6 using glacial acetic acid, and the mixture was then stirred and heated at 90 °C for 2 h under a nitrogen atmosphere. After cooling to room temperature, the suspension was washed sequentially with deionized water (3 × 500 mL), methanol (3 × 300 mL), and deionized water (5 × 500 mL). The silica magnetite composite was stored in deionized water at a concentration of 40.0 g L<sup>-1</sup>.

The protection of the silica film on Fe<sub>3</sub>O<sub>4</sub> particles was judged by the leaching concentrations of total iron ions (TOT[Fe]) from the prepared particles in the acidic solution. The particle was placed in the 0.01 mol L<sup>-1</sup> hydrochloric acid solution at a ratio of mass to volume equal to 1 g L<sup>-1</sup>. After shaking for 20 h at 150 rpm and 298 K, the particles were separated by magnet and then filtrated through a 0.22 μm pore size membrane. TOT[Fe] in the filtrate was determined by the ICP-OES analysis. The well protection of silica film was ensured as the value of TOT[Fe] of filtrate was lower than the value of method determination limits.

### 2.5. Preparation of L grafted Fe<sub>3</sub>O<sub>4</sub>/SiO<sub>2</sub>

A 25 mL of silica-coated magnetite solution prepared as described above was washed with ethanol (3 × 50) mL and then homogeneously dispersed to 100 mL with 5% L in hot ethanol and 8 mmol L<sup>-1</sup> acetic acid solution (pH 4.5). The solution was transferred into a 250 mL 3-necked round-bottom flask and ultrasonicated for 30 min. Then, the mixture was stirred and heated at 60 °C for 2 h. After that, the resulting modified nanoparticles were washed three times with deionized water and two times with methanol, and then dried at room temperature under vacuum situation.

### 2.6. Extraction and desorption procedure

For the extraction and preconcentration of analytes in aqueous sample, a series of sample solutions containing Pb(II), Cd(II) and Cu(II) were transferred into a 500 mL beaker. The pH of the solution was adjusted to 7.0 using 0.01–0.1 mol L<sup>-1</sup> HCl and/or NaOH solutions. Then, 0.13 g of adsorbent was added, and the solution was ultrasonicated for 10 min to facilitate adsorption of the metal ions on the nanoparticles. Then the magnetic adsorbent was collected at the bottom of beaker by the application of an external field on the outside of the beaker via a piece of permanent magnet, and the supernatant was decanted directly. The magnet was removed, and a solution containing a mixture of 3.0 mL of 1.0 mol L<sup>-1</sup> HNO<sub>3</sub> and 1.0 mL of methanol was added as eluent and ultrasonicated again for 2 min. Finally, the magnet was used again to settle the nanoparticles, and the eluent was transferred into a test tube for subsequent FAAS analysis (Fig. 1).

### 2.7. Preparation of real samples

In order to demonstrate the applicability and reliability of the method for real world samples, seven samples, including tap water, petrochemical wastewater, tuna fish, shrimp, rice, tobacco and hair samples were prepared and analyzed by the method.

Tap water samples were taken from our research laboratory (Bu-Ali Sina University, Hamedan, Iran) without pretreatment before determination, the pH value was adjusted at 7.0 with 0.01–0.1 mol L<sup>-1</sup> HCl and/or NaOH and the preconcentration/separation procedure was performed.

Petrochemical wastewater samples were collected in a 2.0 L PTFE bottle and filtered through a filter paper (Whatman No. 40) before use.

The proposed method was applied to determine lead, cadmium and copper in tuna fish and shrimp samples. Tuna fish and shrimp samples were purchased from a local fish market. 500 mg of dried samples were placed in a digestion vessel and 5 mL of HNO<sub>3</sub> (70%) plus 6 mL of H<sub>2</sub>O<sub>2</sub> (30%) were added. The vessel was immediately assembled, gently swirled and placed in the pre-heated oven at 180 °C for about 1.5 h [28,29]. Then 6 mL of 1 mol L<sup>-1</sup> of K<sub>2</sub>S<sub>2</sub>O<sub>8</sub> was added and heated for 30 min. The digested samples were cooled at room temperature. Appropriate amounts of 2 mol L<sup>-1</sup> NaOH were added to neutralize the excess HNO<sub>3</sub> and then the pH was adjusted at the optimum value. An aliquot of the solution was treated under recommended procedure.

For the determination of Pb(II), Cd(II) and Cu(II) in tobacco samples, the samples (500 mg) were accurately weighted into the PTFE high-pressure microwave acid-digestion vessels, and 3.0 mL of concentrated nitric acid plus 5.0 mL of 30% hydrogen peroxide were added. The vessels were sealed tightly and then positioned in the carousel of the microwave oven. The system was operated at full power for 8.0 min. The digest was evaporated to near dryness. The residue was dissolved with 5 mL of 5% (m/v) nitric acid, and quantitatively transferred into a 50 mL volumetric flask for further analysis [30].

For rice samples (imported rice to Iran), 1.0 g of the sample was weighed and powdered. Then 15 mL of concentrated HNO<sub>3</sub> was added and the mixture was kept overnight. Then, 6 mL of concentrated HNO<sub>3</sub> and 4 mL of concentrated HClO<sub>4</sub> were added to the beaker. It was evaporated near to dryness on a hot plate at about 130 °C for 3 h. The residue was dissolved in 0.5 mol L<sup>-1</sup> HNO<sub>3</sub> and filtered. The clear solution obtained was diluted to 50 mL with distilled water [11].

An amount of approximately 100–300 mg of hair was sampled for each subject from the occipital zone of the head at 1 cm from the scalp by using surgical scissors with tungsten carbide covered cutting edges, in order to avoid sample contamination from metals released through the friction exerted during sampling. Samples were then placed in polyethylene bags and stored in a desiccator in dark until analysis. To remove the external contamination from hair samples, the pre-digestion washing technique should be such that it would only remove the surface external contamination without extracting metals from samples or depositing metals on them. Hair samples were washed with acetone-deionized water-deionized water-deionized water-acetone as recommended by international atomic energy agency [31]. The washed samples were placed in glass beakers individually and allowed to dry at room temperature. Decomposition of organic matter is an important part for determination of heavy metals in hair samples. A 100 mg of the washed sample was weighed and transferred to a beaker. To decompose the hair samples a mixture of nitric acid and hydrogen peroxide (2:1) is sufficient. In this acid digestion system, samples were decomposed at 150 °C temperature for approximately 1 h in the closed beaker.

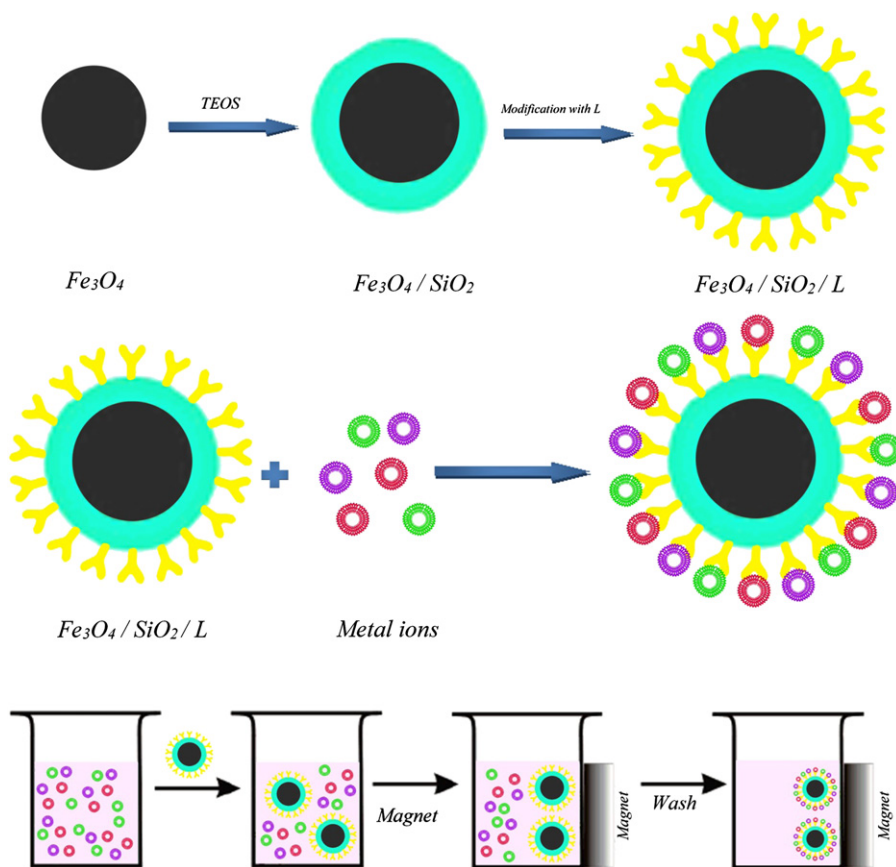


Fig. 1. Procedure for synthesizing Schiff base modified silica-coated magnetic nanoparticles and for the proposed magnetic solid-phase extraction.

### 3. Results and discussion

#### 3.1. Characteristics of prepared nano-solid phase

The particle size and morphology of  $\text{Fe}_3\text{O}_4$ ,  $\text{Fe}_3\text{O}_4/\text{SiO}_2$  and  $\text{Fe}_3\text{O}_4/\text{SiO}_2/\text{L}$  were evaluated from TEM micrographs. The average diameter of  $\text{Fe}_3\text{O}_4$  nanoparticles is 26 nm with a spherical shape in Fig. 2(a), and the aggregation of the nanoparticles can be discerned clearly. In Fig. 2(b), the coated silica layer as the typical core-shell structure of the  $\text{Fe}_3\text{O}_4/\text{SiO}_2$  nanoparticles can be observed. The dispersity of  $\text{Fe}_3\text{O}_4/\text{SiO}_2$  nanoparticles is also improved, and the average size is increased to about 38 nm. The modification of the  $\text{Fe}_3\text{O}_4/\text{SiO}_2$  nanoparticles with L does not result in the change of the morphology and size of the obtained  $\text{Fe}_3\text{O}_4/\text{SiO}_2/\text{L}$  (Fig. 2(c)), but the aggregation of the  $\text{Fe}_3\text{O}_4$  nanoparticles is more evident than that of  $\text{Fe}_3\text{O}_4/\text{SiO}_2$  nanoparticles.

The typical XRD profile of magnetite and silica coated magnetite nanoparticles is shown in Fig. 3(a) and (b), respectively. The XRD pattern of the magnetite exactly matched the Joint Committee on Powder Diffraction Standards (JCPDS) reference no. 19-629. The XRD patterns of  $\text{Fe}_3\text{O}_4/\text{SiO}_2$  and  $\text{Fe}_3\text{O}_4/\text{SiO}_2/\text{L}$  are similar to that of  $\text{Fe}_3\text{O}_4$  nanoparticles. The peak at around  $2\theta=20^\circ$  in the XRD pattern (Fig. 3(b)) is due to the amorphous silica shell on the surface of the magnetite nanoparticles. However, the characteristic diffraction peaks of  $\text{Fe}_3\text{O}_4$  are weakened because of the silica coat and the mixed group modification, and the diffraction peak of amorphous silica can be observed. Also, with comparison of peaks of silica-coated magnetite nanoparticles and silica-coated magnetite nanoparticles modified with L concluded although the magnetic particle surfaces were coated with L, the very distinguishable FCC peaks of magnetite crystal were observable, which means that these particles have the phase stability. The different

functional groups of L did not affect on crystallinity and morphology in this study [32].

The FT-IR spectra of  $\text{Fe}_3\text{O}_4$ ,  $\text{Fe}_3\text{O}_4/\text{SiO}_2$ , L and  $\text{Fe}_3\text{O}_4/\text{SiO}_2/\text{L}$  are shown in Fig. 4. The synthesized  $\text{Fe}_3\text{O}_4$  nanoparticles can be seen from the occurrence of a strong absorption band in the FT-IR spectrum, which encompasses the characteristic wavenumbers of 625 and 575  $\text{cm}^{-1}$  (Fig. 4(a)). This pattern corresponds to the Fe–O bonds, which is reported to belong to bulk magnetite. In addition, the final product obtained from the coprecipitation was dense, black and magnetic implying the presence of magnetite as the main phase. The deposition of silica network on the magnetite surface by Fe–O–Si bonds through silanization was also confirmed by obtaining relevant FT-IR spectrum. The corresponding absorption band cannot be seen in the FT-IR spectrum because it appears at around 580  $\text{cm}^{-1}$  and inevitably overlaps with the Fe–O vibration of magnetite [15,23,33]. However, the strongly absorbing region of 1020–1110  $\text{cm}^{-1}$  in the spectrum of Fig. 4(b) results from the vibration of Si–O–H and Si–O–Si groups.

As it can be seen, S–H bond stretching vibration around 2033  $\text{cm}^{-1}$  and C–N bond stretching vibration around 1391  $\text{cm}^{-1}$  were clearly observed in the FT-IR spectrum of  $\text{Fe}_3\text{O}_4/\text{SiO}_2/\text{L}$ , the N–H stretching and bending vibrations at 1478 and 3312  $\text{cm}^{-1}$  demonstrate the successful modification indicating that L has been successfully loaded on the self-prepared  $\text{Fe}_3\text{O}_4$  magnetic nanoparticles [15,21,23].

Also, the specific surface area of the prepared nanoparticles is determined by the physical adsorption of a gas on the surface of the solid, by measuring the amount of adsorbed gas corresponding to a monomolecular layer on the surface. The data are treated according to the BET theory [34]. The results of the BET method showed that the average specific surface areas of  $\text{Fe}_3\text{O}_4$  MNPs, silica-coated MNPs and silica-coated MNPs modified with Schiff

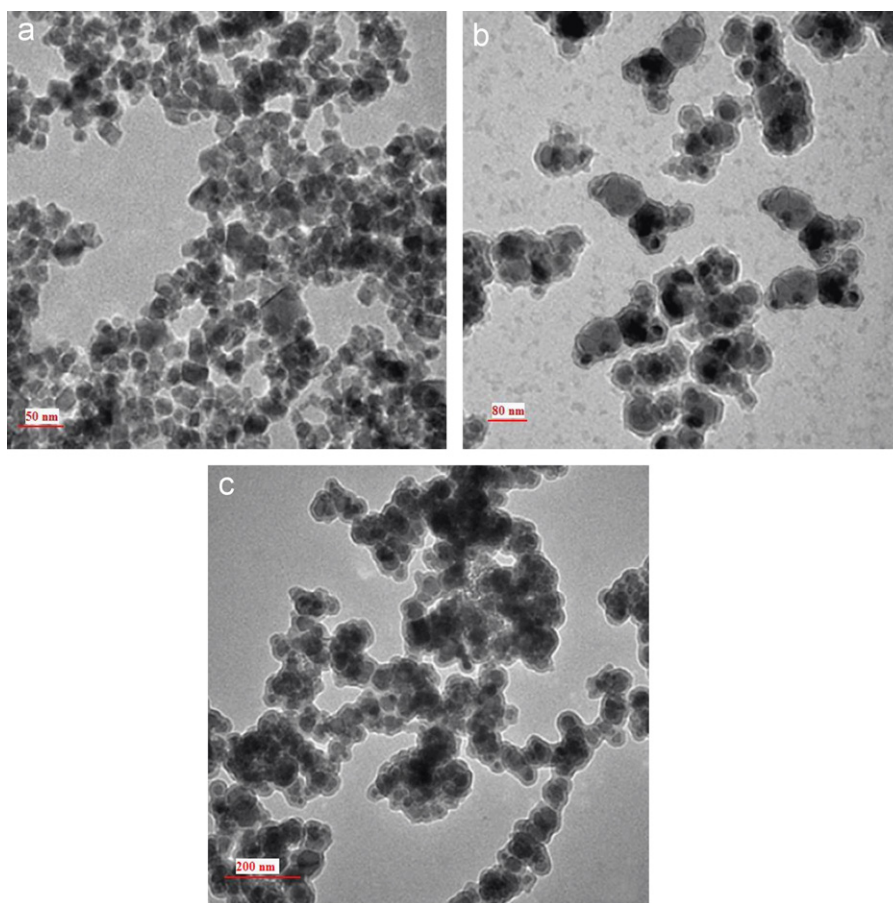


**Fig. 2.** TEM images of Fe<sub>3</sub>O<sub>4</sub> (a), Fe<sub>3</sub>O<sub>4</sub>/SiO<sub>2</sub> (b), and Schiff base modified Fe<sub>3</sub>O<sub>4</sub>/SiO<sub>2</sub> (c).

base were 105.6, 109.1 and 106.4 m<sup>2</sup> g<sup>-1</sup>, respectively. It can be concluded from these values that the synthesized nanoparticles have relatively large specific surface areas. It can also be seen that the specific surface areas were not obviously different for Fe<sub>3</sub>O<sub>4</sub>, Fe<sub>3</sub>O<sub>4</sub>/SiO<sub>2</sub> and Fe<sub>3</sub>O<sub>4</sub>/SiO<sub>2</sub>/L. Therefore, the process of silanization and modification do not influence the characteristics of the sorbents and the differences in the subsequent study between them cannot be attributed to the morphological differences.

### 3.2. Point of zero charge of nanoparticles

The isoelectric point (iep) is an important characteristic of metal oxides. Surface charge of oxides due to hydroxyl groups is largely dependent on the pH of the solution, the pH<sub>PZC</sub> caused by the amphoteric behavior of hydroxylated surface groups and the interaction between surface sites and the electrolyte species. In this study, the iep of the bare and finalized magnetite NPs was determined in degassed 0.01 mol L<sup>-1</sup> NaNO<sub>3</sub> solutions, at 20 °C. Given volume (30 mL) of 0.01 mol L<sup>-1</sup> NaNO<sub>3</sub> solutions were taken and mixed with 30 mg of NPs, in different beakers. The pH values of the solutions were adjusted to 2, 3, 4, 5, 6, 7, 8, 9 using solutions of HNO<sub>3</sub> and NaOH. The initial pH of the solution was recorded and each flask was covered with parafilm and shaken for 24 h. The final pH values of the solutions were recorded and the difference between initial and final pH – the so-called ΔpH – was plotted against the initial pH values. The iep values were calculated from ΔpH versus pH plots, at the pH where ΔpH=0 [23,33]. The iep of Fe<sub>3</sub>O<sub>4</sub> MNPs is consistent with the reported value at pH 6.5. The iep of silica-coated MNPs was 3.28, and it approached to the reported value of natural silica which is 3.0 [23,33]. The iep of Fe<sub>3</sub>O<sub>4</sub>/SiO<sub>2</sub>/L was at about pH 3.8.

The surface charge is positive at pH values lower than pH<sub>PZC</sub>, neutral at pH<sub>PZC</sub>, and negative at pH values higher than it. Surface coverage of the magnetite with silica, reasonably, leads to a decrease in the pH<sub>PZC</sub> of the surface approaching the respective value of pure silica. Differences reported in the synthesis procedures, aqueous medium conditions and measuring methods are likely to be the cause of the different pH<sub>PZC</sub>. Actually, lower concentrations of TEOS in the silanization procedure described above, gave rise to higher pH<sub>PZC</sub> for the produced silica-coated magnetite. The incomplete surface coating results in a non-homogeneous surface chemical composition, which affects the pH<sub>PZC</sub> of the silanized magnetite.

### 3.3. Variables affecting the preconcentration process

To demonstrate that the method allowed an efficient extraction of trace amounts of Pb(II), Cd(II) and Cu(II), the extraction and elution procedure was optimized to achieve quantitative recovery. The optimization involved testing different conditions of extraction pH, sample volume, eluent composition, elution volume, extraction, elution and sedimentation time for metal-adsorbent complexes, and interference effects from other ions.

#### 3.3.1. Effect of pH

In the solid phase extraction studies for heavy metal ions, the influence of pH of the aqueous solution is one of the main factors for quantitative recoveries of the analytes. An appropriate pH value could improve the adsorption efficiency, and also reduce interference from the matrix. As could be seen in Fig. 5 and with attention to iep value of adsorbent, the adsorption percentage of

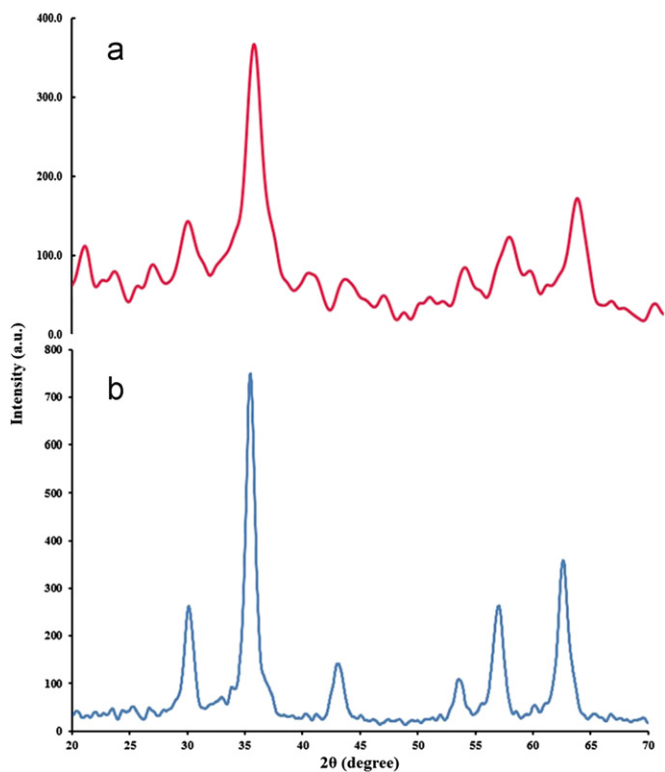


Fig. 3. XRD patterns of Fe<sub>3</sub>O<sub>4</sub> nanoparticles (a) and Fe<sub>3</sub>O<sub>4</sub>/SiO<sub>2</sub> (b).

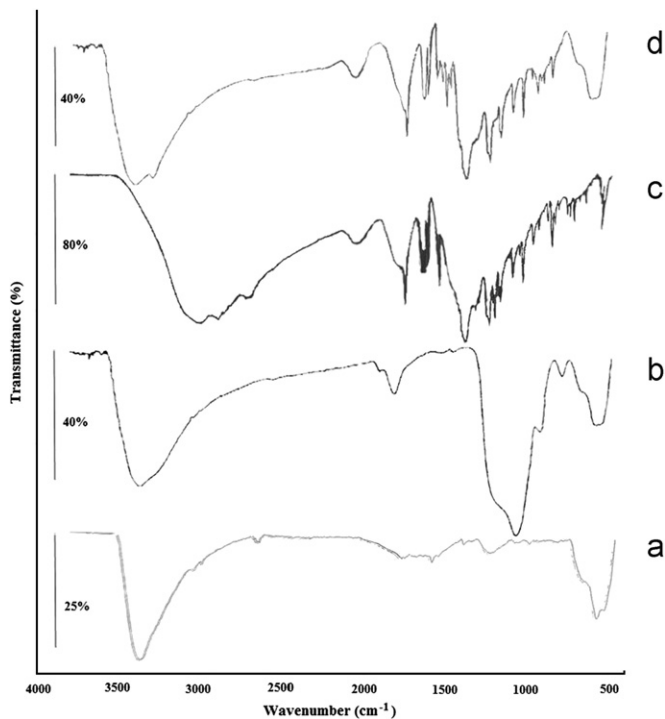


Fig. 4. FT-IR spectra of Fe<sub>3</sub>O<sub>4</sub> (a), Fe<sub>3</sub>O<sub>4</sub>/SiO<sub>2</sub> (b), Schiff base (c), Fe<sub>3</sub>O<sub>4</sub>/SiO<sub>2</sub>/Schiff base (d).

Pb(II), Cd(II) and Cu(II) increased by increasing the aqueous solution pH from 2.0 to 7.0, and a quantitative adsorption for the analytes was obtained at pH 7.0. When pH was further increased from 7.0 to 9.0, the adsorption percentage for the target analytes kept almost constant. Considering that the —S—H group

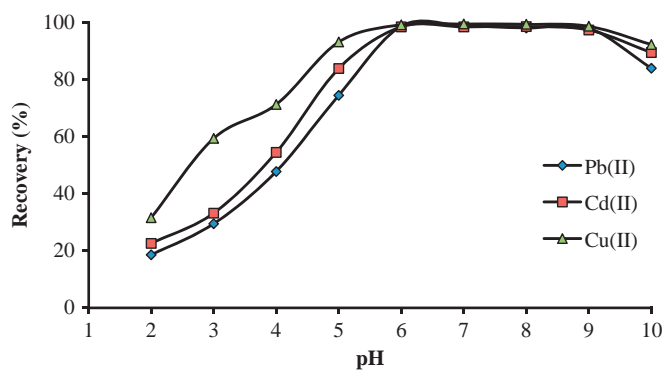


Fig. 5. Effect of the pH on the recovery percentage of metal ions by Fe<sub>3</sub>O<sub>4</sub>/SiO<sub>2</sub>/L sorbent. Conditions: 100 mL of 10 μg L<sup>-1</sup> of metal ions, 0.15 g of adsorbent; eluent: 3.0 mL of 1.0 mol L<sup>-1</sup> HNO<sub>3</sub> and 1.0 mL of methanol, ultrasonication time: 12 min.

could be oxidized if the Fe<sub>3</sub>O<sub>4</sub>/SiO<sub>2</sub>/L were stored in acidic media for a long time, pH 7.0 was selected for subsequent experiments.

The lower the solution pH value is, the more easily N with one electron pair will bind with H, C–N will break and electron provided by C will transfer to form other bond. As pH increases, the L tended more to exist in natural form, which would easily form complex with metal ions through the functional sites. This may be attributed to the presence of free lone pair of electrons on nitrogen and sulfur atoms, which are suitable functional sites for coordination with the metal ions. However, the precipitation of metal ions would occur when pH value was too high. Therefore, neutral and weakly alkaline sample solution is preferred for the extraction of target metal ions.

### 3.3.2. Effect of the adsorbent amount

The amount of adsorbent is another important parameter to obtain quantitative recovery. For this reason the amounts of silica-coated magnetite nanoparticles modified with L was optimized. Nanoparticles have been used as better sorbents for their high surface areas than conventional sorbents. Therefore, fewer amounts of nano-sorbents can achieve satisfactory results. The influence of the adsorbent amount was tested in the range 0.03–0.15 g. According to the results, quantitative recoveries were obtained when nano-sized adsorbent amount was above 0.13 g (Fig. 6). Therefore, 0.13 g of adsorbent was used in all experiments.

### 3.3.3. Effect of type and volume of eluent on recovery

To obtain a high enrichment factor, a suitable eluent should be used. The eluent should elute the sorbed analytes quantitatively in a small volume. It should also not affect the accurate determination of the analytes and destroy the life time and reusability of solid phase. Fig. 5 shows that the sorption of cations at pH < 3.0 is negligible, one can expect that elution may be favored in acidic solutions. So various acidic solutions were used for desorption of the studied ions following the recommended procedure. The experimental results indicated that a mixture of 3.0 mL of 1.0 mol L<sup>-1</sup> HNO<sub>3</sub> and 1.0 mL of methanol was an efficient eluent and also a suitable matrix for determination of analytes by FAAS. The effect of eluent volume was also evaluated by eluting target metal ions with four replicate of the mixture of 1.0 mol L<sup>-1</sup> HNO<sub>3</sub> and methanol sequentially, and it was found that the mixture of 2.0 mL of 1.0 mol L<sup>-1</sup> HNO<sub>3</sub> and 1 mL of methanol could fulfill the quantitative recovery of target metal ions. In order to prevent possible error caused by small volume solution introduction in FAAS, the mixture of 3.0 mL of 1.0 mol L<sup>-1</sup> HNO<sub>3</sub> and 1.0 mL of methanol was used for the elution of the adsorbed metal ions in subsequent experiments.

### 3.3.4. Effect of sample volume

In order to obtain a higher enrichment factor, a large volume of sample solution is required. It was found that quantitative recoveries for all target analytes were obtained when sample volumes were less than 350 mL. Hence, sample volume of 350 mL was selected for subsequent experiments.

### 3.3.5. Effect of ultrasonication time

In the SPE process, the contact time is one of the prime factors influencing the target analytes extraction. The results showed when the adsorbent was isolated immediately without a contact process into the samples, the analytes were hardly adsorbed. Ultrasonication caused an increase in the adsorption and desorption rates. Ultrasonic times for adsorption and elution were also optimized in order to minimize the time required for sample processing. The experimental results indicated that quantitative recovery of all analytes in 350 mL sample solution was achieved when the ultrasonication time was greater than 8 min for adsorption and greater than 1.5 min for elution. Subsequent experiments used ultrasonication times of 10 min for adsorption and 2 min for elution.

### 3.3.6. Effect of sediment time

The effect of sediment time on the recovery of metal ions was investigated, and no significant effect was observed when the sedimentation time was greater than 1 min. A sediment time of 1 min was therefore selected in subsequent experiments. Meanwhile, in the experiments,  $\text{Fe}_3\text{O}_4/\text{SiO}_2/\text{L}$  possessed super paramagnetic properties and large saturation magnetization, which enabled them to be completely isolated in a short amount of time (less than

1 min) by a strong magnet. In a word, analysis time is shortened greatly compared to the traditional column-passing SPE.

### 3.4. Coexisting ions interference

With attention to provide high selectivity using flame atomic absorption spectrometry, the only interference may be attributed to the preconcentration step. Under the optimized experimental conditions, the interference of coexisting ions on the recovery of metal ions (at  $10 \mu\text{g L}^{-1}$  level of each target metal ion) was investigated. The results showed that the recoveries for the target analytes could remain above 95% even in the presence of  $3 \text{ g L}^{-1} \text{K}^+$  and  $\text{Na}^+$ ,  $2 \text{ g L}^{-1} \text{Ca}^{2+}$  and  $\text{Mg}^{2+}$ ,  $0.5 \text{ g L}^{-1} \text{NH}_4^+$ ,  $0.1 \text{ g L}^{-1} \text{Fe}^{3+}$ ,  $0.01 \text{ g L}^{-1} \text{Al}^{3+}$ ,  $\text{Mn}^{2+}$ ,  $\text{Co}^{2+}$  and  $\text{Ni}^{2+}$ ,  $8 \text{ g L}^{-1} \text{SO}_4^{2-}$ ,  $4 \text{ g L}^{-1} \text{Cl}^-$  and  $6 \text{ g L}^{-1} \text{NO}_3^-$ , respectively, indicating that the developed method has a good tolerance to matrix interference.

### 3.5. Analytical figures of merit

Under the optimum conditions described above, calibration curves were constructed for the determination of Pb(II), Cd(II) and Cu(II) ions according to the general procedure. Linearity was maintained between 0.32–320.0, 0.63–300.0 and 0.28–400.0  $\mu\text{g L}^{-1}$  for Pb(II), Cd(II) and Cu(II), in a 350 mL sample. The detection limit was determined as three times of the standard deviation (11 replicate measurements) of blank sample. The detection limits of this method, in the original solution, for the determination of Pb(II), Cd(II) and Cu(II) ions were 0.14, 0.19 and 0.12  $\mu\text{g L}^{-1}$ , respectively. This detection limit could be improved if other techniques like: ICP-OES-MS or ETAAS are used. However, for the aims of the present work FAAS proved to be adequate.

As mentioned previously, the amount of target ions in 350 mL was measured after elution of adsorbed ions by 4.0 mL of eluent, therefore the maximum preconcentration factors for this method is 87.5.

Seven replicate determinations of metal ions after preconcentration of 50 mL of mixture of  $2.50 \mu\text{g L}^{-1}$  of Pb(II), Cd(II) and Cu(II) ions gave a relative standard deviations of 1.4, 1.6 and 1.8%, respectively. Calibration slopes increased proportionally to increase the concentrated volume, which indicates that the retention/elution efficiency of the process is constant ( $\sim 100\%$ ).

### 3.6. Analysis of the real samples

The method was applied to the determination of trace amounts of Pb(II), Cd(II) and Cu(II) ions in a wide variety of samples. The samples were also analyzed after spiking with different concentrations of

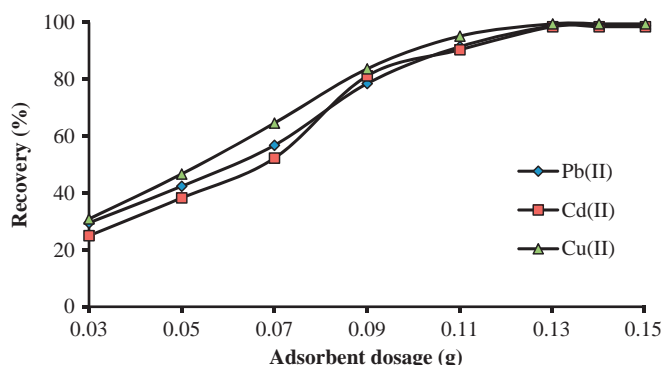


**Fig. 6.** Effect of the adsorbent amount on extraction of metal ions by  $\text{Fe}_3\text{O}_4/\text{SiO}_2/\text{L}$ . Conditions: 100 mL of  $10 \mu\text{g L}^{-1}$  of metal ions, pH=7, eluent: 3.0 mL of  $1.0 \text{ mol L}^{-1} \text{HNO}_3$  and 1.0 mL of methanol, ultrasonication time: 12 min.

**Table 1**

Results of target ions determination in various water samples using  $\text{Fe}_3\text{O}_4/\text{SiO}_2/\text{L}$  sorbent under the optimum conditions ( $N=5$ ).

Sample	Analyte	Added ( $\mu\text{g L}^{-1}$ )	Found ( $\mu\text{g L}^{-1}$ )	Recovery (%)	ICP-AES method	$t_{\text{exp}}^a$
Tap water	Pb(II)	0.00	$6.10 \pm 0.05^b$	–	$6.15 \pm 0.07$	1.55
		20.00	$25.82 \pm 0.02$	98.6	$25.80 \pm 0.06$	0.83
	Cd(II)	0.00	$0.97 \pm 0.04$	–	$0.94 \pm 0.02$	1.87
		20.00	$21.13 \pm 0.04$	100.8	$21.18 \pm 0.09$	1.11
	Cu(II)	0.00	$14.65 \pm 0.05$	–	$14.73 \pm 0.04$	2.27
		20.00	$35.04 \pm 0.02$	102.0	$34.96 \pm 0.11$	1.95
Petrochemical wastewater	Pb(II)	0.00	$23.47 \pm 0.04$	–	$23.40 \pm 0.01$	1.71
		10.00	$33.62 \pm 0.02$	101.5	$33.67 \pm 0.06$	0.29
	Cd(II)	00.00	$10.35 \pm 0.05$	–	$10.42 \pm 0.07$	2.17
		10.00	$20.51 \pm 0.04$	101.6	$20.58 \pm 0.09$	2.06
	Cu(II)	0.00	$31.38 \pm 0.04$	–	$31.36 \pm 0.10$	0.52
		10.00	$41.26 \pm 0.02$	98.8	$41.24 \pm 0.01$	2.00

<sup>a</sup>  $t_{\text{exp}}$  shows the experimental student —  $t$  values, ( $t_{8,0.05}=2.31$ ).

<sup>b</sup> Mean of five determinations ( $t_{4,0.05}=2.78$ ).

**Table 2**  
Results of target ions determination in various real samples using Fe<sub>3</sub>O<sub>4</sub>/SiO<sub>2</sub>/L sorbent under optimum conditions (N=5).

Sample	Analyte	Added (ng g <sup>-1</sup> )	Found (ng g <sup>-1</sup> )	Recovery (%)	ICP-OES method	t <sub>exp</sub> <sup>b</sup>
Tuna fish	Pb(II)	0.00	8.36 ± 0.36 <sup>a</sup>	–	8.42 ± 0.29	0.36
		10.00	18.65 ± 0.21	102.9	18.71 ± 0.25	0.53
	Cd(II)	0.00	5.60 ± 0.19	–	5.48 ± 0.20	0.79
		10.00	15.72 ± 0.15	101.2	15.61 ± 0.17	1.34
	Cu(II)	0.00	61.50 ± 0.06	–	61.47 ± 0.11	0.65
		10.00	71.36 ± 0.05	98.6	71.30 ± 0.09	1.67
Shrimp	Pb(II)	0.00	42.20 ± 0.11	–	42.26 ± 0.14	0.95
		10.00	52.08 ± 0.11	98.8	52.05 ± 0.09	0.59
	Cd(II)	0.00	25.48 ± 0.19	–	25.30 ± 0.27	1.51
		10.00	35.62 ± 0.14	101.4	35.57 ± 0.16	1.97
	Cu(II)	0.00	85.19 ± 0.07	–	85.25 ± 0.06	1.71
		10.00	95.45 ± 0.07	102.6	95.53 ± 0.10	1.78
Rice	Pb(II)	0.00	37.94 ± 0.06	–	38.10 ± 0.21	2.02
		10.00	47.72 ± 0.08	97.8	47.83 ± 0.17	1.57
	Cd(II)	0.00	3.68 ± 0.07	–	3.75 ± 0.10	1.55
		10.00	13.55 ± 0.06	98.7	13.63 ± 0.07	2.29
	Cu(II)	0.00	2.24 ± 0.11	–	2.27 ± 0.12	0.50
		10.00	12.20 ± 0.12	99.6	12.15 ± 0.12	0.79
Tobacco	Pb(II)	0.00	3.26 ± 0.12	–	3.20 ± 0.16	0.82
		10.00	13.32 ± 0.09	100.6	13.35 ± 0.09	0.68
	Cd(II)	0.00	9.91 ± 0.10	–	9.81 ± 0.07	2.22
		10.00	19.86 ± 0.06	99.5	19.95 ± 0.05	2.10
	Cu(II)	0.00	12.40 ± 0.09	–	12.46 ± 0.06	1.58
		10.00	22.57 ± 0.07	101.7	22.62 ± 0.04	1.67
Human hair	Pb(II)	0.00	30.15 ± 0.07	–	30.08 ± 0.10	1.55
		10.00	40.28 ± 0.06	101.3	40.32 ± 0.14	0.74
	Cd(II)	0.00	75.33 ± 0.09	–	75.25 ± 0.10	1.70
		10.00	85.19 ± 0.06	98.6	85.17 ± 0.10	0.48
	Cu(II)	0.00	57.04 ± 0.05	–	57.09 ± 0.05	1.75
		10.00	67.26 ± 0.04	102.2	67.25 ± 0.04	0.53

<sup>a</sup> Mean of five determinations (t<sub>4,0.05</sub> = 2.78).

<sup>b</sup> t<sub>exp</sub> shows the experimental student — t values, (t<sub>8,0.05</sub> = 2.31).

**Table 3**  
Comparative data from some recent papers on solid-phase extraction.

Analytical technique	Metal ions	Target analyte	Dynamic range (µg L <sup>-1</sup> )	Detection limit (µg L <sup>-1</sup> )	Precision (% RSD)	Ref.
DNPH-nano-γ-Al <sub>2</sub> O <sub>3</sub> -FAAS	Pb and Cr	Pb(II)	1.2–350	0.43	1.4 <sup>a</sup>	[11]
		Cd(II)	–	–	–	
		Cu(II)	–	–	–	
Fe <sub>3</sub> O <sub>4</sub> /SiO <sub>2</sub> /SA-FAAS	Cr, Cu, Ni and Cd	Pb(II)	–	–	–	[21]
		Cd(II)	0.37–450.0	0.11	2.6 <sup>b</sup>	
		Cu(II)	0.73–400.0	0.22	2.2	
DZ-MNP-ICP-OES	Cr, Cu, Pb and Zn	Pb(II)	0.5–100.0	0.062	3.1 <sup>c</sup>	[35]
		Cd(II)	–	–	–	
		Cu(II)	0.1–100.0	0.011	2.4	
HPAPyr-XAD-2-FAAS	Cu, Zn, Pb and Cd	Pb(II)	3–1000	2.8	–	[36]
		Cd(II)	2–1250	0.9	–	
		Cu(II)	10–1000	2.0	–	
MSPE-ICP-OES	Ag, Cd, Cu and Zn	Pb(II)	–	–	–	[37]
		Cd(II)	–	0.12	4.03 <sup>d</sup>	
		Cu(II)	–	0.13	3.62	
Sulfur-nanoparticle-FAAS	Cd, Cu, Zn, and Pb	Pb(II)	1.0–60.0	0.63	4.8 <sup>e</sup>	[38]
		Cd(II)	0.8–30.0	0.30	2.4	
		Cu(II)	0.5–40.0	0.24	2.0	
Fe <sub>3</sub> O <sub>4</sub> /SiO <sub>2</sub> /Schiff base-FAAS	Pb, Cd and Cu	Pb(II)	0.32–320.0	0.14	1.4 <sup>f</sup>	This work
		Cd(II)	0.63–300.0	0.19	1.6	
		Cu(II)	0.28–400.0	0.12	1.8	

<sup>a</sup> For the determination of 100.0 µg L<sup>-1</sup> (n=7).

<sup>b</sup> Not available.

<sup>c</sup> For the determination of 10.0 µg L<sup>-1</sup> (n=7).

<sup>d</sup> For the n=5.

<sup>e</sup> For the n=8.

<sup>f</sup> For the determination of 2.5 µg L<sup>-1</sup> (n=7).



analytes. Tap water, petrochemical wastewater, tuna fish, shrimp, rice, tobacco and human hair samples were analyzed. The analytical results are presented in Tables 1 and 2. In view of the high selectivity provided by flame atomic absorption spectrometry, the recovery of spiked samples is satisfactory (in the range 97.8–102.9%), which indicates the capability of the system in the determination of analytes in real samples with different matrices. Also, the target ions in the samples were determined by ICP-OES. For comparing the results of the suggested method with those of ICP-OES, we applied the t-test to compare the results. It can be concluded from Tables 1 and 2 that there is no significant difference between the results obtained by the two methods for  $P=0.05$ . The results show that the method is suitable for the analysis of real samples.

#### 4. Conclusions

A selective and sensitive solid-phase preconcentration method for the determination of Pb(II), Cd(II) and Cu(II) ions was developed. The feasibility of the method was demonstrated by application to seven different natural samples and waters. The novel synthesized and characterized L coated silica magnetite phase for the preconcentration is highly advantageous compared to the other materials due to rapidity and high selectivity for analytes. Hence, the proposed method substantially lowers the risk of contamination. It is also highly sensitive, selective, simple, and robust to use, cost-effective, and eco-friendly. Compared with the recently reported methods, better figures of merit and recoveries were obtained for target analytes [11,21,33,35–38]. The comparison of the results is given in Table 3.

#### Acknowledgment

The authors are very grateful to the Research Council of Science and Research Branch, Islamic Azad University for financial support. Further, the authors thank Dr. Masoumeh Tabatabaee (Yazd Branch, Islamic Azad University, Yazd) for guidance about the preparation of the Schiff base. Also, for performing the TEM measurements, we thank Dr. P. Shahbazikhah (USA), and M. Daryanavard and F. Fazlali for their assistance with sampling.

#### References

[1] L. Zhou, C. Gao, W.J. Xu, ACS Appl. Mater. Interfaces 2 (2010) 1483–1491.

- [2] J.W. Hamilton, R.C. Kaltreider, O.V. Bajenova, M.A. Ihnat, J. McCaffrey, B.W. Turpie, E.E. Rowell, J. Oh, M.J. Nemeth, C.A. Pesce, J.P. Lariviere, J. Environ. Health 106 (1998) 1005–1015.
- [3] B.L. Vallee, D.D. Ulmer, Annu. Rev. Biochem. 41 (1972) 91–128.
- [4] T. Partanen, P. Heikkila, S. Hernberg, T. Kauppinen, G. Moneta, A. Ojarvi, Scand. J. Work Environ. Health 17 (1991) 231–239.
- [5] G. Aragay, J. Pons, A. Merkoci, Chem. Rev. 111 (2011) 3433–3458.
- [6] C. Duran, D. Ozdes, D. Sahin, V.N. Bulut, A. Gundogdu, M. Soylak, Microchem. J. 98 (2011) 317–322.
- [7] M. Soylak, A. Aydin, Food Chem. Toxicol. 49 (2011) 1242–1248.
- [8] A. Karatepe, M. Soylak, L. Elci, Clean, Soil, Air, Water 39 (2011) 502–507.
- [9] M. Soylak, E. Yilmaz, Desalination 275 (2011) 297–301.
- [10] A. Afkhami, T. Madrakian, H. Siampour, J. Hazard. Mater. 138 (2006) 269–272.
- [11] A. Afkhami, M. Saber-Tehrani, H. Bagheri, T. Madrakian, Microchim. Acta 172 (2011) 125–136.
- [12] A. Karatepe, M. Soylak, L. Elci, Talanta 85 (2011) 1974–1979.
- [13] A. Afkhami, T. Madrakian, R. Ahmadi, H. Bagheri, M. Tabatabaee, Microchim. Acta 175 (2011) 69–77.
- [14] J.S. Suleiman, B. Hu, X. Pu, C.Z. Huang, Z.C. Jiang, Microchim. Acta 159 (2007) 379–385.
- [15] C.Z. Huang, B. Hu, Spectrochim. Acta B 63 (2008) 437–444.
- [16] A. Kraus, K. Jainae, F. Unob, N. Sukpirom, J. Colloid Interface Sci. 338 (2009) 359–365.
- [17] A.H. Lu, E.L. Salabas, F. Schuth, Angew. Chem. Int. Ed. 46 (2007) 1222–1244.
- [18] A. Afkhami, R. Norooz-Asl, Colloids Surf., A 346 (2009) 52–57.
- [19] A. Afkhami, R. Moosavi, J. Hazard. Mater. 174 (2010) 398–403.
- [20] A. Afkhami, R. Moosavi, T. Madrakian, Talanta 82 (2010) 785–789.
- [21] M.R. Shishehbore, A. Afkhami, H. Bagheri, Chem. Cent. J. 5 (2011) 41–51.
- [22] A. Afkhami, M. Saber-Tehrani, H. Bagheri, Desalination 263 (2010) 240–248.
- [23] X.O. Zhang, H.Y. Niu, Y.Y. Pan, Y. Shi, Y. Cai, J. Colloid Interface Sci. 362 (2011) 107–112.
- [24] F. Shemirani, A.A. Mirroshandel, M. Salavati-Niasari, R.R. Kozani, J. Anal. Chem. 59 (2004) 228–233.
- [25] D. Kara, A. Fisher, S.J. Hill, J. Hazard. Mater. 165 (2009) 1165–1169.
- [26] M. Tabatabaee, M.M. Heravi, M. Sharif, F. Esfandiyari, E.-J. Chem. 8 (2011) 535–540.
- [27] X.Q. Liu, Z.Y. Ma, J.M. Xing, H.Z. Liu, J. Magn. Magn. Mater. 270 (2004) 1–6.
- [28] K. Helrich, Official Methods of Analysis, Association of Official Analytical Chemists (AOAC), 1990 p.1.
- [29] F.A. Silva, I.L. Alcantara, P.S. Roldan, Florentino, P.M. Padilha, Eclética Quim. 30 (2005) 47.
- [30] W.Z. Yang, Q. Hu, J. Ma, L. Wang, G.G. Yang, G. Xie, J. Braz. Chem. Soc. 17 (2006) 1039–1044.
- [31] International Atomic Energy Agency (IAEA), Report on the Second Research Co-Ordination Meeting of IAEA, Neuherberg, Germany, 1985.
- [32] S.I. Park, J.H. Kim, J.H. Lim, C.O. Kim, Curr. Appl Phys. 8 (2008) 706–709.
- [33] A.E. Karatapanis, Y. Fiamegos, C.D. Stalikas, Talanta 84 (2011) 834–839.
- [34] S. Brunauer, P.H. Emmett, E. Teller, J. Am. Chem. Soc. 60 (1938) 309–319.
- [35] G.H. Cheng, M. He, H.Y. Peng, B. Hu, Talanta 88 (2012) 507–515.
- [36] N. Burham, S.A. Azeem, M.F. El-Shahat, Cent. Eur. J. Chem. 7 (2009) 945–954.
- [37] M.H. Mashhadizadeh, Z. Karami, J. Hazard. Mater. 190 (2011) 1023–1029.
- [38] K. Ghanemi, Y. Nikpour, O. Omidvar, A. Maryamabadi, Talanta 85 (2011) 763–769.